Journal of Nuclear Medicine, published on March 19, 2021 as doi:10.2967/jnumed.120.257345

Dynamic ^{18}F-FPCIT PET: Quantification of Parkinson's disease metabolic networks and nigrostriatal dopaminergic dysfunction in a single imaging session

Shichun Peng[1], Chris Tang[1], Katharina Schindlbeck[1], Yaacov Rydzinski[2,#], Vijay Dhawan[1], Phoebe G. Spetsieris[1], Yilong Ma[1,*], David Eidelberg[1,*]

[1]Center for Neurosciences, Institute of Molecular Medicine, The Feinstein Institutes for Medical Research, Northwell Health, Manhasset, NY, USA.

[2]Department of Radiology, Icahn School of Medicine at Mount Sinai, New York, NY, USA.

Running title: Dual-phase ^{18}F-FPCIT PET imaging in PD

*These authors shared senior authorship

Correspondence: Yilong Ma, PhD

Center for Neurosciences, Institute of Molecular Medicine, the Feinstein Institutes for Medical Research, 350 Community Drive, Manhasset, NY 11030, USA. Tel: 516-562-1057, Fax: 516-562-1008. Email: yma@northwell.edu

The first author: Shichun Peng, PhD

The same affiliation, address and contact information. Email: speng@northwell.edu

#Present address: University Radiology Group, 579A Cranbury Rd, East Brunswick, NJ 08816

Word Counts: 6800

Funding: Supported by NIH grant (P50 NS 071675 to DE).

Abstract

Previous multi-center imaging studies with ^{18}F-FDG PET have established the presence of Parkinson's disease motor- and cognition-related metabolic patterns termed PDRP and PDCP in patients with this disorder. Given that in PD cerebral perfusion and glucose metabolism are typically coupled in the absence of medication, we determined whether subject expression of these disease networks can be quantified in early-phase images from dynamic ^{18}F-FPCIT PET scans acquired to assess striatal dopamine transporter (DAT) binding. **Methods:** We studied a cohort of early-stage PD patients and age-matched healthy control subjects who underwent ^{18}F-FPCIT at baseline; scans were repeated 4 years later in a smaller subset of patients. The early ^{18}F-FPCIT frames, which reflect cerebral perfusion, were used to compute PDRP and PDCP expression (subject scores) in each subject, and compared to analogous measures computed based on ^{18}F-FDG PET scan when additionally available. The late ^{18}F-FPCIT frames were used to measure caudate and putamen DAT binding in the same individuals. **Results:** PDRP subject scores from early-phase ^{18}F-FPCIT and ^{18}F-FDG scans were elevated and striatal DAT binding reduced in PD versus healthy subjects. The PDRP scores from ^{18}F-FPCIT correlated with clinical motor ratings, disease duration, and with corresponding measures from ^{18}F-FDG PET. In addition to correlating with disease duration and analogous ^{18}F-FDG PET values, PDCP scores correlated with DAT binding in the caudate/anterior putamen. PDRP and PDCP subject scores using either method rose over 4 years whereas striatal DAT binding declined over the same time period. **Conclusion:** Early-phase images obtained with ^{18}F-FPCIT PET can provide an alternative to ^{18}F-FDG PET for PD network quantification. This technique therefore allows

PDRP/PDCP expression and caudate/putamen DAT binding to be evaluated with a single tracer in one scanning session.

Key words: Parkinson's disease, cerebral perfusion, metabolic networks, dual-phase imaging, ^{18}F-FPCIT PET, ^{18}F-FDG PET

Introduction

Parkinson's disease (PD) is characterized by widespread disruption in regional cerebral glucose metabolism and blood flow in response to degeneration of the nigrostriatal dopamine system and related pathways. Over the last two decades, a wide variety of imaging biomarkers have been developed for PD by measuring: (A) striatal binding of presynaptic and postsynaptic dopaminergic markers such as dopamine transporter (DAT) and D_2 receptor using radioligands with both PET and SPECT; (B) regional brain metabolism with ^{18}F-FDG PET; and (C) regional brain perfusion with PET, SPECT and arterial spin labeling (ASL) MRI. Dopaminergic markers measure highly localized neurochemical deficits in the brain, whereas regional metabolism and blood flow provide versatile markers of functional activity at the network level (*1-4*).

It has been shown with ^{18}F-FDG PET in American populations that motor and cognitive dysfunction in PD are associated with highly reproducible disease-related metabolic covariance patterns termed PDRP (*5*) and PDCP (*6*), both of which have since been replicated in multiple patient cohorts scanned in a variety of independent imaging centers in Asia and Europe (*4,7-11*). Expression levels for the PDRP and PDCP in individual patients (subject scores) correlate with individual differences in motor and cognitive dysfunction. These measures increase with disease progression, and correlate with striatal presynaptic dopaminergic markers in both cross-sectional (*10,12,13*) and longitudinal (*14*) investigations. More specifically, PDRP and PDCP expression values have been found respectively to correlate with dopaminergic activity in the posterior putamen and in the caudate and anterior putamen in a PET study using both ^{18}F-FDG and ^{18}F-FDOPA in the same patients (*15*). Indeed, subject scores for these patterns have been used to

assess rates of disease progression and treatment responses in PD without the floor effects seen with presynaptic dopaminergic imaging markers (*16*).

PDRP and PDCP subject scores can be measured in cerebral blood flow (CBF) images obtained with $H_2{}^{15}O$ PET and correlate strongly with analogous scores in concurrent ^{18}F-FDG PET scans in patients with PD (*5,17*). These early reports established high reproducibility of PDRP and PDCP subject scores in test-retest studies with both CBF and metabolic images regardless of clinical stages and treatment status. This suggests that perfusion scans can substitute for ^{18}F-FDG PET because of the tight coupling between these tracers that exists in the absence of dopaminergic medication at the regional and network levels (*18,19*).

Subsequent studies have revealed that early-phase scans from dynamic PET imaging of dopaminergic tracers such as ^{11}C-raclopride provide measures of cerebral perfusion that can complement striatal D2 receptor binding measurements from late-phase data (*20*). Indeed, a dynamic PET study with DAT radioligands such as ^{11}C-PE2I or ^{18}F-FPCIT can provide a powerful alternative to dual-tracer or dual-modality examinations such as ^{123}I-FPCIT SPECT and ^{18}F-FDG PET used for the differential diagnosis of parkinsonism (*21,22*). To date, however, it is unclear whether such early-phase scans can be used (instead of ^{18}F-FDG PET) to quantify PDRP and PDCP expression of patients and healthy control subjects.

In this PET study, we determined: (1) Whether PDRP and PDCP expression levels can be quantified with early-phase ^{18}F-FPCIT scans. Can these measurements accurately discriminate PD patients from healthy control subjects? (2) How well these measures correlate with independent clinical ratings of disease severity; (3) How well these values compared with corresponding expression levels determined independently with ^{18}F-FDG PET in the same subjects; (4) The relationships between pattern expression and caudate/putamen DAT binding

measurements obtained with dynamic ^{18}F-FPCIT PET in the same scanning session; and (5) How well these pattern expression measures can track changes associated with disease progression.

Methods

Human Subjects

Patients with early-stage Parkinson's disease (PD) without dyskinesia (n = 25) and age-matched normal control (NL) subjects (n = 16) underwent dynamic ^{18}F-FPCIT PET described elsewhere (*12*). In PD patients, imaging was conducted in the fasting state, at least 12 hours after the last dose of anti-parkinsonian medication; prior to imaging, patients were evaluated clinically according to Hoehn and Yahr (HY) stage and the Unified Parkinson's Disease Rating Scale (UPDRS III). Clinical and demographic details for these subjects are provided in Table 1. Of these participants, a subgroup of 18 PD and 7 NL subjects was additionally studied with ^{18}F-FDG PET under similar scan conditions, conducted within approximately one month of ^{18}F-FPCIT PET. Of the patients scanned with ^{18}F-FPCIT and ^{18}F-FDG PET, eight were rescanned after an average of four years (mean between-session interval: 46.4 ± 14.7 months). The study was approved by the institutional review board of North Shore University Hospital. All subjects gave written informed consent following detailed explanation of the imaging procedures. The study had also been done in compliance with the Health Insurance Portability and Accountability Act.

Dual-tracer PET imaging

PET imaging studies were performed in 3-dimensional (3D) mode on a GE Advance camera at North Shore University Hospital. ^{18}F-FPCIT images were acquired in dynamic mode over 0-100 min post-injection (see below). ^{18}F-FDG images were obtained in static mode over 35-45 min post-injection on separate days. Both images were reconstructed using a 3D reprojection algorithm following attenuation correction with PET transmission scan collected for each emission imaging session. Dynamic ^{18}F-FPCIT frames and static ^{18}F-FDG images were separately processed according to analytical protocols established at our center (*5,23*). Images of DAT binding were generated by specific uptake ratio measured in late-phase ^{18}F-FPCIT PET defined by (voxel count/occipital count -1) between 90-100 min post-injection. Striatal DAT binding was then measured on a hemispheric basis and averaged in caudate nucleus, putamen and its subdivisions by using customized volumes of interest (VOIs) for each subject. The same set of VOIs was projected onto the images of DAT binding in the analysis of the subject at follow-up. All dynamic ^{18}F-FPCIT frames (via early-phase data) and ^{18}F-FDG images were spatially normalized to the PET template in SPM (Wellcome Department of Imaging Neurosciences, Institute of Neurology, London, UK) implemented in Matlab 7.3.0 (Mathworks Inc, Sherborn, MA) and smoothed with a 3D Gaussian kernel of 10-mm width to enhance signal-to-noise over the whole brain.

Network Expression

PDRP/PDCP expression levels (subject scores) were computed in early-phase dynamic ^{18}F-FPCIT PET scan frames, and in the static ^{18}F-FDG images as described in detail elsewhere (*2,24*). These computations utilized an automated, voxel-based algorithm and were conducted blind to subject category (PD/NL), radiotracer (^{18}F-FPCIT/^{18}F-FDG), and time window/point

(see below). For all scans, subject scores were standardized (*z*-scored) with respect to the mean and standard deviation (SD) of the healthy control group. The software used for these calculations is freely available at http://www.feinsteinneuroscience.org/. To determine the optimal time window for early-phase imaging, we used linear interpolation to divide imaging frames of variable duration over the first 10-min after ^{18}F-FPCIT injection into 10 individual frames of 1-min duration and computed PDRP/PDCP subject scores individually for each frame (Supplementary Fig. 1; Supplementary Tables 1-2). This procedure also mitigated the effects of unequal framing in dynamic acquisitions commonly performed in clinical practice. Mean subject scores were then calculated by averaging over a scan duration of 2, 5 and 10 min respectively. Composite images (Fig. 1) were also displayed as the weighted average over the same frames to visualize regional cerebral perfusion across subject groups.

Statistical Analysis

Differences between two independent groups or changes within-subject between two dependent variables were assessed by unpaired and paired Student's *t*-tests, respectively. Differences in network expression values (subject scores) computed over the three specified ^{18}F-FPCIT time windows, or in the rates of longitudinal change were compared using one- and two-way repeated measures analysis of variance (RMANOVA) models. Relationships between variables within-subject were evaluated in each group by Pearson correlation coefficients. Data analysis was conducted using SPSS software (SPSS Inc., Chicago, IL) running on Windows Virtual PC with the level of significance set at $P < 0.05$.

Results

Optimal time window

PDRP subject scores computed in the individual 1-min frames over the first 10 min following ^{18}F-FPCIT injection provided similar discrimination of PD versus healthy control subjects (Supplementary Fig. 1 and Supplementary Tables 1-2). Additionally, network correlations of PDRP and PDCP scores with motor ratings, disease duration, and analogous ^{18}F-FDG PET measures were of comparable magnitude across the individual frames. Longitudinal changes in subject scores over the 4-year follow-up period were also similar for the various frames. The optimal time window was determined by comparing the performance of subject scores computed for dynamic acquisitions of varying length over the initial 10 min (Supplementary Table 3 and Tables 2-3).

Disease discrimination

Brain perfusion images from early-phase dynamic ^{18}F-FPCIT scans averaged over the first 2-, 5- and 10-min post-injection were similar to corresponding ^{18}F-FDG images in both PD patients and NL subjects (Fig. 1). The accuracy of group separation and longitudinal change for the various network expression measurements and for caudate/putamen DAT binding are summarized in Supplementary Table 3. Subject scores were elevated in PD versus NL groups for PDRP ($P < 0.04$, unpaired *t*-tests) but not for PDCP ($P \geq 0.32$) in each of the three early-phase ^{18}F-FPCIT images (Fig. 2A, B). Subject scores in PD patients obtained with ^{18}F-FDG were also elevated for PDRP ($P < 0.02$) but did not reach significance for PDCP ($P = 0.11$). Computed

PDRP subject scores did not differ significantly for the three different early-phase ^{18}F-FPCIT time windows ($P = 0.82$; one-way RMANOVA). No significant differences were seen between early-phase ^{18}F-FPCIT subject scores for each time window and corresponding ^{18}F-FDG PET measures ($P \geq 0.15$; paired *t*-tests). Differences in corresponding PDCP values did not reach significance across time windows ($P = 0.12$; one-way RMANOVA), but were lower for each ^{18}F-FPCIT time window compared to ^{18}F-FDG PET ($P < 0.025$; paired *t*-tests). By contrast, striatal DAT binding (Fig. 2C) was reduced ($P < 0.001$, unpaired *t*-tests) in the PD relative to NL groups and did not differ for left and right striatal regions in the patient and NL groups ($P \geq 0.15$, paired *t*-tests). The reduction was greater from the caudate to the anterior and posterior axis of the putamen ($P < 0.0001$).

In summary, subject scores measured with dynamic ^{18}F-FPCIT PET between 0-10 min were more sensitive to discriminate groups by PDRP (PD vs. NL) and to detect longitudinal changes by both PDRP and PDCP (4 years vs. baseline in PD) compared to the composite 2-min and 5-min early-phase scans (Supplementary Table 3). We therefore reported the remaining results based on the composite 10-min frame.

Clinical correlations

PD patients showed strong intercorrelations between clinical HY stage, UPDRS motor ratings and disease duration ($r \geq 0.700$, $P < 0.0001$); age did not correlate with the other variables ($r \leq 0.28$, $P \geq 0.18$). Off-state UPDRS motor ratings in PD patients correlated with PDRP subject scores computed over the first 10-min after ^{18}F-FPCIT injection ($r = 0.439$, $P = 0.028$;

Supplementary Fig. 2A), but the correlation with PDCP scores did not reach significance in the same time window ($r = 0.339$, $P = 0.10$; Supplementary Fig. 2C). Clinical motor ratings did not correlate with DAT binding measured for the caudate, putamen, and the putamen subregions (Supplementary Table 4). Disease duration correlated with PDRP ($r = 0.409$, $P = 0.042$; Supplementary Fig. 2B) and PDCP ($r = 0.457$, $P = 0.022$; Supplementary Fig. 2D) subject scores computed for the 10-min frame, and with putamen DAT binding ($r = -0.419$, $P = 0.037$; Supplementary Fig. 3).

Relationships between ^{18}F-FPCIT and ^{18}F-FDG PET imaging markers

We found significant correlations between PDRP subject scores in PD measured by the two methods ($r = 0.863$, $P < 0.0001$; Fig. 3A); analogous subject scores correlations were also seen for PDCP ($r = 0.675$, $P < 0.005$; Fig. 3B). Moreover, within-modality correlations (Supplementary Table 5) were detected between PDRP and PDCP values measured with early-phase ^{18}F-FPCIT PET in PD patients ($r = 0.750$, $P < 0.0001$; Fig. 3C) and NL subjects ($r = 0.879$, $P < 0.00001$; Supplementary Fig. 4A) and with ^{18}F-FDG PET in PD patients ($r = 0.713$, $P = 0.001$; Supplementary Fig. 4B). In late-phase scans, DAT binding were significantly correlated for the caudate and putamen, and across putamen subregions (PD: $r \geq 0.594$, $P \leq 0.002$; NL: $r \geq 0.931$, $P < 0.0001$; Supplementary Table 4). Nonetheless, caudate and putamen DAT binding correlations with PDRP subject scores computed in the early-phase scans were not significant ($|r| \leq 0.356$; $P \geq 0.10$; Table 2). However, PDCP expression computed in the early-phase scans exhibited a negative correlation (Table 3) with DAT binding in the caudate and the anterior putamen ($r = -0.404$, $P < 0.05$; Fig. 3D). By contrast, PDCP correlations with DAT

binding measured in the whole putamen or in the middle and posterior putamen subregions did not reach significance ($|r| \leq 0.386$, $P \geq 0.06$).

Disease progression

Brain perfusion images from early-phase dynamic ^{18}F-FPCIT scans were similar to corresponding ^{18}F-FDG images in PD at baseline and follow-up (Supplementary Fig. 5). Robust increases in HY clinical stages and motor ratings (Table 1) were recorded in the group of eight PD patients who underwent longitudinal imaging over the 46-month period ($P < 0.001$, paired *t*-test). The accuracy of longitudinal change for various network scores and for caudate/putamen DAT binding are presented in Supplementary Table 3. Expression levels for the both PDRP and PDCP increased (Fig. 4A-D) over time in early-phase ^{18}F-FPCIT PET ($P < 0.01$ for each pattern), as well as in ^{18}F-FDG PET (PDRP: $P < 0.0005$; PDCP: $P < 0.02$; paired *t*-tests). Conversely, the corresponding striatal DAT binding values in this PD subgroup decreased from baseline in both putamen and caudate nucleus ($P < 0.05$; Fig. 4E, F). Moreover, the rates of longitudinal changes did not significantly differ for PDRP and PDCP subject scores, or for putamen and caudate DAT binding, estimated respectively using early- and late-phase ^{18}F-FPCIT PET ($P > 0.10$, 2 × 2 RMANOVA). By contrast, changes in subject scores were greater with ^{18}F-FDG PET as compared to the corresponding values obtained using early-phase ^{18}F-FPCIT PET, reaching significance for PDRP ($P = 0.004$) but not for PDCP ($P = 0.182$). The changes in subject scores were also greater for PDRP than for PDCP with ^{18}F-FDG PET ($P = 0.035$).

No correlations were detected between longitudinal changes in the imaging variables and motor ratings ($|r| \leq 0.362$, $P \geq 0.38$) or between-scan interval ($|r| \leq 0.441$, $P \geq 0.27$). Interval changes demonstrated strong correlations in PDRP or PDCP subject scores between the 5 min and 10 min frames in early-phase ^{18}F-FPCIT ($r \geq 0.965$, $P < 0.0001$) and in striatal DAT binding

values between putamen and caudate in late-phase ^{18}F-FPCIT ($r = 0.812$, $P = 0.014$). By contrast, significant correlations were not present between interval changes in PDRP and PDCP expression measured with early-phase ^{18}F-FPCIT or ^{18}F-FDG PET ($r \leq 0.536$, $P \geq 0.17$). Likewise, the changes recorded with the early-phase ^{18}F-FPCIT did not correlate with analogous changes with ^{18}F-FDG PET or with changes in striatal DAT binding recorded using the late-stage ^{18}F-FPCIT scans ($|r| \leq 0.482$, $P \geq 0.27$).

Discussion

In this study, we found that PDRP expression levels measured in early-phase ^{18}F-FPCIT PET scans discriminated patients with early-stage PD from age-matched normal control subjects with similar accuracy for the first 2, 5 and 10 min of the dynamic ^{18}F-FPCIT PET acquisitions. This level of discrimination was also detected using corresponding values obtained concurrently with ^{18}F-FDG PET in a smaller sample of PD and control subjects, as reported previously in similar early-stage PD cohorts (*25-28*). On the other hand, PDCP expression values did not discriminate patients and healthy control subjects scanned with either ^{18}F-FPCIT or ^{18}F-FDG PET, consistent with the relatively intact cognitive function seen in these early-stage patients. That said, expression levels for both networks measured in early-stage PD patients with the early-phase ^{18}F-FPCIT images exhibited strong correlations with corresponding values from ^{18}F-FDG PET. Of note, the strength of these subject score correlations were comparable to those observed in PD patients scanned with both $H_2{}^{15}O$ and ^{18}F-FDG PET in the resting state (*5,17*) and in others who underwent dual modality imaging with ASL MRI and ^{18}F-FDG PET (*8,29*).

We also found that PDRP expression levels measured in early-stage PD patients using early-phase ^{18}F-FPCIT PET (2, 5 and 10 min) correlated with independent motor ratings, in

keeping with previously published ^{18}F-FDG PET studies (*1,7,9,27*). Accordingly, analogous correlations with motor disability were not seen for PDCP subject scores computed in the same subjects (*1,11,30*). Along these lines, PDRP and PDCP expression levels computed in early-phase ^{18}F-FPCIT PET scans correlated with disease duration. Moreover, significant increases in these measures were seen over time in patients scanned longitudinally by this method, at rates comparable to those assessed using ^{18}F-FDG PET for network quantification (*16*). Nonetheless, given the small sample size we were underpowered to detect any correlations between the changes in these brain network markers and clinical motor ratings.

On the other hand, symmetrical and significant reductions of DAT binding were seen in the caudate and putamen, and in putamen subregions in late-phase ^{18}F-FPCIT PET scans from the same patients. In accord with prior studies, reductions in putamen DAT binding were seen with increasing disease duration [e.g., (*31*)]. It is noteworthy that individual differences in caudate and anterior putamen DAT binding correlated with PDCP (but not PDRP) expression levels measured in the early-phase ^{18}F-FPCIT PET scans. This underscores the role of these regions in mediating cognitive dysfunction in non-demented PD patients (*12,15,32*).That said, significant correlations were not observed between PDRP expression and putamen DAT binding. This was likely attributable to the lower signal and incipient floor effects noted in this region even in early-stage PD patients (*14,33*). While caudate and putamen DAT binding declined significantly over the four-year longitudinal study, the changes were small compared to the increases in PDRP and PDCP expression seen concurrently in the same subjects. This difference and the relatively small sample size may account for the absence of correlations between interval changes in the imaging measures.

PDRP and PDCP expression values can be reliably quantified in early-phase ^{18}F-FPCIT PET scan data using computational methods similar to those employed with ^{18}F-FDG PET. Indeed, the early-phase measurements were quite stable in discriminating early-stage PD from healthy control subjects and in assessing longitudinal changes in scans acquired over the initial 10 min post-injection (Supplementary Tables 1-2). Likewise, correlations of PDRP and PDCP subject scores with motor ratings and disease duration, and with corresponding FDG PET measurements were maintained over each of the 1-min frames. Indeed, these findings are consistent with the performance of the composite frames obtained over the first 2, 5, and 10 min after injection.

Our results further indicate that early-phase ^{18}F-FPCIT PET images recorded over the first 10-min are superior for assessing PDRP and PDCP expression in individual patients. This is likely due to the higher signal-to-noise ratio inherent in the long time-frame images. Indeed, these scans exhibited stronger correlations with corresponding expression values from ^{18}F-FDG PET, as well as with UPDRS motor ratings (Tables 2-3; cf., Fig. 3 and Supplementary Fig. 2). In this regard, the findings are in line with previously reported regional data (*22*). Moreover, the 10-min time window provided useful network measurements even after omitting the first 1-min, 2-min, or even 5-min of the acquisition (Supplementary Tables 6-8).

It has been reported that early-phase data of many specific PET radioligands mimic brain perfusion in healthy subjects and in patients with neurodegenerative disorders. This had been validated in PET imaging studies of Alzheimer's disease [e.g., (*34,35*)]. Early-phase data from dopaminergic PET tracers such as ^{18}F-FDOPA (*15*), ^{11}C-raclopride (*20*), or DAT tracers such as ^{11}C-PE2I (*21*) can similarly be used to compute PDRP and PDCP expression in individual

subjects. Dual-phase imaging with these tracers may offer the advantage of network quantification and dopaminergic assessments in a single PET session.

This study was limited in several ways. Because only a portion of the current sample was imaged with both tracers, we were unable to rigorously compare the early- and late-phase ^{18}F-FPCIT measurements with ^{18}F-FDG PET subject scores from the same individuals. Although PDRP scores in the early-phase ^{18}F-FPCIT data were comparable to ^{18}F-FDG PET, analogous PDCP scores from ^{18}F-FPCIT tended to be somewhat lower particularly when integrating the frames over a longer duration. Whether ^{18}F-FDG PET is more sensitive to gauging PDCP expression values when compared to ^{18}F-FPCIT PET remains to be investigated by assessing the strength and reliability of their neuropsychological correlates in PD patients with cognitive dysfunction. That said, PDRP/PDCP subject scores computed in early-phase ^{18}F-FPCIT PET scans replicated the previous findings in PD reported in many prior studies on this topic with ^{18}F-FDG PET (see the specific discussions above).

The use of dynamic ^{18}F-FPCIT PET may help in the evaluation of antiparkinsonian treatments in which nigrostriatal dopamine function is improved along with downstream changes in disease networks such as PDRP. For example, in an ^{18}F-FDG PET study of retinal pigmented epithelial (RPE) cells implanted in the putamen of parkinsonian non-human primates, we found that expression levels for the parkinsonism-related pattern (PRP, homologous to the PDRP in human PD) (*36,37*) were reduced by treatment (*38*). Conceivably, this change can be captured using early-phase ^{18}F-FPCIT PET, while quantifying potential changes in dopaminergic innervation through late-phase imaging. Whereas cell-based interventions such as RPE cell implantation will not necessarily alter striatal DAT binding, dynamic ^{18}F-FPCIT PET may be appropriate for disease-modifying interventions such as the induction of growth factors in the

putamen (*39*). Moreover, concurrent measurements of disease network expression in early-phase data can improve the accuracy of differential diagnosis based on clinical assessments with or without adjunctive dopaminergic imaging (*10,40-42)*. This hybrid approach may be especially useful in screening potential participants in trials of new interventions for PD and related disorders.

We wish to emphasize that in this study, early-phase ^{18}F-FPCIT PET scans were used solely to quantify expression levels for the two validated disease-related metabolic networks, namely PDRP and PDCP. We did not interrogate other patient populations to see whether early-phase dynamic acquisitions appropriately captured other disease-related covariance patterns such as those reported previously for multiple system atrophy (MSA), progressive supranuclear palsy (PSP), and corticobasal degeneration (CBD) (*43,44*). It is also worth noting that while regional and network-level measurements of CBF and glucose metabolism are coupled in healthy subjects and in early-stage PD patients scanned off medication, significant dissociation between these measures occurs during dopaminergic treatment (*18,19*). Uncoupling effects of this sort are particularly prominent in brain regions such as the putamen in which dopaminergic afferents are present to both neurons and blood vessels (*45*). Lastly, network approaches have recently been used to map specific treatment-induced metabolic patterns for investigational purposes [e.g., (*46*)]. It is unclear at present, however, whether early-phase scans have sufficient power to capture stable network topographies of this sort. Further studies with both tracers will be needed to address these issues.

Conclusion

Dual-phase ^{18}F-FPCIT PET is a viable methodology for quantitative assessment of PD-related metabolic brain networks and presynaptic nigrostriatal dopaminergic functioning in a single imaging session. The ability to measure PDRP and PDCP expression levels and caudate/putamen DAT binding in individual patients following the injection of a single radiotracer represents a substantial saving in time, cost, and patient convenience.

Acknowledgments

This work was supported by the U.S. National Institute of Neurological Disorders and Stroke (P50 NS 071675 [Morris K. Udall Centre of Excellence for Parkinson's Disease Research at The Feinstein Institutes for Medical Research] to D.E.). The content is solely the responsibility of the authors and does not necessarily represent the official views of the National Institutes of Health or the National Institute of Neurological Disorders and Stroke. The authors thank Yoon Young Choi for her valuable editorial assistance preparing the manuscript.

Disclosure

The authors have no conflict of interest to report. Dr. Eidelberg serves on the scientific advisory board and has received honoraria from The Michael J. Fox Foundation for Parkinson's Research; serves on the scientific advisory board and receives personal fees from Ovid Therapeutics; has received consultant fees from MeiraGTx; is listed as co-inventor of patents re: Markers for use in screening patients for nervous system dysfunction and a method and apparatus for using same, without financial gain; and has received research support from the NIH (NINDS NIDCD, NIAID) and the Dana Foundation.

Key Points

QUESTION: Previous multi-center imaging studies with ^{18}F-FDG PET have established the presence of motor- and cognition-related metabolic patterns (i.e., PDPR and PDCP) in Parkinson's disease. We determined whether subject expression scores of these disease-related brain networks can be measured in early-phase images from dynamic ^{18}F-FPCIT PET scans used to assess striatal DAT binding. We also examined how these measures compare with analogous network scores obtained with currently acquired ^{18}F-FDG PET scans and clinical indicators of disease severity and duration.

PERTINENT FINDINGS: PDRP scores from early-phase ^{18}F-FPCIT images and ^{18}F-FDG scans were both elevated along with reduced striatal DAT binding in PD patients versus healthy control subjects. The PDRP scores from ^{18}F-FPCIT correlated with severity of clinical motor symptoms while both PDRP and PDCP scores correlated with disease duration and more strongly with analogous brain network scores from ^{18}F-FDG in the same patients. The PDCP scores from ^{18}F-FPCIT data also correlated with DAT binding in caudate/anterior putamen. Moreover, the corresponding PDRP and PDCP scores from both early-phase ^{18}F-FPCIT and ^{18}F-FDG images increased with striatal DAT binding further decreased from baseline in a subset of PD patients with follow-up.

IMPLICATIONS FOR PATIENT CARE: This work shows that one can evaluate both brain network expression scores related with motor and cognition dysfunction and abnormal caudate/putamen DAT binding in PD with a single tracer in one scanning session. The method can be used to improve the outcomes of patient care and clinical research studies by increasing

the throughput in nuclear medicine centers with minimum radiation exposure. A dynamic or dual-phase ^{18}F-FPCIT PET imaging protocol may be more valuable to fully characterize neuropathophysiology and evaluate disease discrimination and progression in parkinsonism.

References

1. Eidelberg D. Metabolic brain networks in neurodegenerative disorders: a functional imaging approach. *Trends Neurosci.* 2009;32:548-557.
2. Spetsieris PG, Eidelberg D. Scaled subprofile modeling of resting state imaging data in Parkinson's disease: methodological issues. *Neuroimage.* 2011;54:2899-2914.
3. Peng S, Eidelberg D, Ma Y. Brain network markers of abnormal cerebral glucose metabolism and blood flow in Parkinson's disease. *Neuroscience bulletin.* 2014;30:823-837.
4. Schindlbeck KA, Eidelberg D. Network imaging biomarkers: insights and clinical applications in Parkinson's disease. *Lancet Neurol.* 2018;17:629-640.
5. Ma Y, Tang C, Spetsieris PG, Dhawan V, Eidelberg D. Abnormal metabolic network activity in Parkinson's disease: test-retest reproducibility. *J Cereb Blood Flow Metab.* 2007;27:597-605.
6. Huang C, Mattis P, Tang C, Perrine K, Carbon M, Eidelberg D. Metabolic brain networks associated with cognitive function in Parkinson's disease. *Neuroimage.* 2007;34:714-723.
7. Wu P, Wang J, Peng S, et al. Metabolic brain network in the Chinese patients with Parkinson's disease based on 18F-FDG PET imaging. *Parkinsonism Relat Disord.* 2013;19:622-627.
8. Teune LK, Renken RJ, de Jong BM, et al. Parkinson's disease-related perfusion and glucose metabolic brain patterns identified with PCASL-MRI and FDG-PET imaging. *Neuroimage Clin.* 2014;5:240-244.
9. Tomse P, Jensterle L, Grmek M, et al. Abnormal metabolic brain network associated with Parkinson's disease: replication on a new European sample. *Neuroradiology.* 2017;59:507-515.
10. Ko JH, Lee CS, Eidelberg D. Metabolic network expression in parkinsonism: Clinical and dopaminergic correlations. *J Cereb Blood Flow Metab.* 2017;37:683-693.
11. Meles SK, Tang CC, Teune LK, et al. Abnormal metabolic pattern associated with cognitive impairment in Parkinson's disease: a validation study. *J Cereb Blood Flow Metab.* 2015;35:1478-1484.
12. Niethammer M, Tang CC, Ma Y, et al. Parkinson's disease cognitive network correlates with caudate dopamine. *Neuroimage.* 2013;78:204-209.
13. Liu FT, Ge JJ, Wu JJ, et al. Clinical, Dopaminergic, and Metabolic Correlations in Parkinson Disease: A Dual-Tracer PET Study. *Clin Nucl Med.* 2018;43:562-571.
14. Huang C, Tang C, Feigin A, et al. Changes in network activity with the progression of Parkinson's disease. *Brain.* 2007;130:1834-1846.
15. Holtbernd F, Ma Y, Peng S, et al. Dopaminergic correlates of metabolic network activity in Parkinson's disease. *Hum Brain Mapp.* 2015;36:3575-3585.
16. Niethammer M, Eidelberg D. Metabolic brain networks in translational neurology: concepts and applications. *Ann Neurol.* 2012;72:635-647.
17. Ma Y, Eidelberg D. Functional imaging of cerebral blood flow and glucose metabolism in Parkinson's disease and Huntington's disease. *Mol Imaging Biol.* 2007;9:223-233.
18. Hirano S, Asanuma K, Ma Y, et al. Dissociation of metabolic and neurovascular responses to levodopa in the treatment of Parkinson's disease. *J Neurosci.* 2008;28:4201-4209.
19. Jourdain VA, Tang CC, Holtbernd F, et al. Flow-metabolism dissociation in the pathogenesis of levodopa-induced dyskinesia. *JCI Insight.* 2016;1:e86615.
20. Van Laere K, Clerinx K, D'Hondt E, de Groot T, Vandenberghe W. Combined striatal binding and cerebral influx analysis of dynamic 11C-raclopride PET improves early

differentiation between multiple-system atrophy and Parkinson disease. *Journal of nuclear medicine : official publication, Society of Nuclear Medicine.* 2010;51:588-595.
21. Appel L, Jonasson M, Danfors T, et al. Use of 11C-PE2I PET in differential diagnosis of parkinsonian disorders. *Journal of nuclear medicine : official publication, Society of Nuclear Medicine.* 2015;56:234-242.
22. Jin S, Oh M, Oh SJ, et al. Additional Value of Early-Phase 18F-FP-CIT PET Image for Differential Diagnosis of Atypical Parkinsonism. *Clinical nuclear medicine.* 2017;42:e80-e87.
23. Ma Y, Dhawan V, Mentis M, Chaly T, Spetsieris PG, Eidelberg D. Parametric mapping of [18F]FPCIT binding in early stage Parkinson's disease: a PET study. *Synapse.* 2002;45:125-133.
24. Peng S, Ma Y, Spetsieris PG, et al. Characterization of disease-related covariance topographies with SSMPCA toolbox: effects of spatial normalization and PET scanners. *Hum Brain Mapp.* 2014;35:1801-1814.
25. Matthews DC, Lerman H, Lukic A, et al. FDG PET Parkinson's disease-related pattern as a biomarker for clinical trials in early stage disease. *Neuroimage Clin.* 2018;20:572-579.
26. Meles SK, Renken RJ, Pagani M, et al. Abnormal pattern of brain glucose metabolism in Parkinson's disease: replication in three European cohorts. *European journal of nuclear medicine and molecular imaging.* 2020; 47:437-450.
27. Schindlbeck KA, Lucas-Jimenez O, Tang CC, et al. Metabolic Network Abnormalities in Drug-Naive Parkinson's Disease. *Mov Disord.* 2020;35:587-594.
28. Tang CC, Holtbernd F, Ma Y, et al. Hemispheric Network Expression in Parkinson's Disease: Relationship to Dopaminergic Asymmetries. *Journal of Parkinson's Disease.* 2020;10:1737-1749.
29. Ma Y, Huang C, Dyke JP, et al. Parkinson's disease spatial covariance pattern: noninvasive quantification with perfusion MRI. *J Cereb Blood Flow Metab.* 2010;30:505-509.
30. Mattis PJ, Niethammer M, Sako W, et al. Distinct brain networks underlie cognitive dysfunction in PD and AD. *Neurology.* 2016;87:1925-1933.
31. Benamer HT, Patterson J, Wyper DJ, Hadley DM, Macphee GJ, Grosset DG. Correlation of Parkinson's disease severity and duration with 123I-FP-CIT SPECT striatal uptake. *Mov Disord.* 2000;15:692-698.
32. Carbon M, Ma Y, Barnes A, et al. Caudate nucleus: influence of dopaminergic input on sequence learning and brain activation in Parkinsonism. *Neuroimage.* 2004;21:1497-1507.
33. Nandhagopal R, Kuramoto L, Schulzer M, et al. Longitudinal progression of sporadic Parkinson's disease: a multi-tracer positron emission tomography study. *Brain : a journal of neurology.* 2009;132:2970-2979.
34. Lopes Alves I, Collij LE, Altomare D, et al. Quantitative amyloid PET in Alzheimer's disease: the AMYPAD prognostic and natural history study. *Alzheimer's Dementia: the journal of the Alzheimer's Association.* 2020;16:750–758.
35. Beyer L, Nitschmann A, Barthel H, et al. Early-phase [18F]PI-2620 tau-PET imaging as a surrogate marker of neuronal injury. *European journal of nuclear medicine and molecular imaging*. 2020; 47:2911–2922.
36. Ma Y, Peng S, Spetsieris PG, Sossi V, Eidelberg D, Doudet DJ. Abnormal metabolic brain networks in a nonhuman primate model of parkinsonism. *J Cereb Blood Flow Metab.* 2012;32:633-642.

37. Ma Y, Johnston TH, Peng S, et al. Reproducibility of a Parkinsonism-related metabolic brain network in non-human primates: A descriptive pilot study with FDG PET. *Movement Disorders.* 2015;30:1283-1288.
38. Peng S, Ma Y, Flores J, et al. Modulation of Abnormal Metabolic Brain Networks by Experimental Therapies in a Nonhuman Primate Model of Parkinson Disease: An Application to Human Retinal Pigment Epithelial Cell Implantation. *J Nucl Med.* 2016;57:1591-1598.
39. Whone A, Luz M, Boca M, et al. Randomized trial of intermittent intraputamenal glial cell line-derived neurotrophic factor in Parkinson's disease. *Brain.* 2019;142:512-525.
40. Rus T, Tomse P, Jensterle L, et al. Differential diagnosis of parkinsonian syndromes: a comparison of clinical and automated - metabolic brain patterns' based approach. *Eur J Nucl Med Mol Imaging.* 2020;47: 2901-2910.
41. Tang CC, Poston KL, Eckert T, et al. Differential diagnosis of parkinsonism: a metabolic imaging study using pattern analysis. *Lancet Neurol.* 2010;9:149-158.
42. Tripathi M, Tang CC, Feigin A, et al. Automated Differential Diagnosis of Early Parkinsonism Using Metabolic Brain Networks: A Validation Study. *Journal of nuclear medicine : official publication, Society of Nuclear Medicine.* 2016;57:60-66.
43. Eckert T, Van Laere K, Tang C, et al. Quantification of Parkinson's disease-related network expression with ECD SPECT. *Eur J Nucl Med Mol Imaging.* 2007;34:496-501.
44. Niethammer M, Tang CC, Feigin A, et al. A disease-specific metabolic brain network associated with corticobasal degeneration. *Brain.* 2014;137:3036-3046.
45. Lerner RP, Francardo V, Fujita K, et al. Levodopa-induced abnormal involuntary movements correlate with altered permeability of the blood-brain-barrier in the basal ganglia. *Scientific reports.* 2017;7:16005.
46. Niethammer M, Tang CC, Vo A, et al. Gene therapy reduces Parkinson's disease symptoms by reorganizing functional brain connectivity. *Sci Transl Med.* 2018;10.

Table 1. Demographic and clinical characteristics of normal control subjects and Parkinson's patients

^{18}F-FPCIT	N	Age (years)	Gender (F/M)	HY Stage	Duration (years)	UPDRS motor
NL	16	52.8 ± 17.1	11/5	NA	NA	NA
PD	25	60.0 ± 10.8	6/19	1.6 ± 1.0	4.8 ± 4.9	12.2 ± 9.6
PD1	8	62.6 ± 7.1	0/8	1.2 ± 0.4	3.0 ± 3.1	8.4 ± 5.1
PD2∗		66.4 ± 7.8		2.2 ± 0.4	6.8 ± 3.5	16.9 ± 5.0
^{18}**F-FDG**						
NL	7	59.3 ± 13.5	3/4	NA	NA	NA
PD	18	60.4 ± 9.0	4/14	1.3 ± 0.4	2.8 ± 1.7	9.4 ± 4.9
PD1	8	59.2 ± 8.0	1/7	1.2 ± 0.4	2.0 ± 1.3	9.6 ± 4.8
PD2∗		63.0 ± 8.4		2.1 ± 0.4	5.8 ± 1.4	17.4 ± 4.9

Data were given as mean ± standard deviations.

NL: normal controls; PD: Parkinson's disease; HY: Hoehn and Yahr; UPDRS: the unified Parkinson's disease rating scale. PD1 and PD2 refer to the baseline and 4-year scans of the longitudinal PD group. Of the eight PD patients with the follow-up, seven had both ^{18}F-FPCIT and ^{18}F-FDG PET while the others underwent imaging with either tracer.

∗ $P < 0.0001$, paired Student's *t*-tests of the follow-up data compared to baseline.

Table 2. Correlations between clinical data and PDRP scores/striatal DAT binding values in Parkinson's patients

	UPDRS	Duration	^{18}F-FPCIT (2 min)	^{18}F-FPCIT (5 min)	^{18}F-FPCIT (10 min)
PDRP scores					
^{18}F-FPCIT (2 min)	0.423 †	0.391			
^{18}F-FPCIT (5 min)	0.438 †	0.407 †	0.983 *		
^{18}F-FPCIT (10 min)	0.439 †	0.409 †	0.954 *	0.992 *	
^{18}F-FDG			0.754 *	0.837 *	0.863 *
Striatal DAT binding					
Caudate			-0.256	-0.290	-0.306
Putamen(whole)			-0.304	-0.301	-0.289
Anterior			-0.270	-0.273	-0.266
Middle			-0.356	-0.351	-0.342
Posterior			-0.319	-0.307	-0.297

Data were Pearson correlation coefficients. PDRP: Parkinson's disease-related pattern; DAT: dopamine transporter binding; UPDRS: the unified Parkinson's disease rating scale.

* $P < 0.0001$,

† $P < 0.05$

Table 3. Correlations between clinical data and PDCP scores/striatal DAT binding values in Parkinson's patients

	UPDRS	Duration	^{18}F-FPCIT (2 min)	^{18}F-FPCIT (5 min)	^{18}F-FPCIT (10 min)
PDCP scores					
^{18}F-FPCIT (2 min)	0.240	0.483 ‡			
^{18}F-FPCIT (5 min)	0.318	0.483 ‡	0.939 *		
^{18}F-FPCIT (10 min)	0.339	0.457 ‡	0.865 *	0.983 *	
^{18}F-FDG			0.510 ‡	0.641 †	0.675 †
Striatal DAT binding					
Caudate			-0.446 ‡	-0.430 ‡	-0.404 ‡
Putamen (whole)			-0.380	-0.345	-0.299
Anterior			-0.481 ‡	-0.419 ‡	-0.365
Middle			-0.386	-0.368	-0.334
Posterior			-0.264	-0.259	-0.237

Data were Pearson correlation coefficients. PDCP: Parkinson's disease cognition-related pattern; DAT: dopamine transporter binding; UPDRS: the unified Parkinson's disease rating scale.

* $P < 0.0001$,

† $P < 0.005$,

‡ $P < 0.05$

Figure Legends

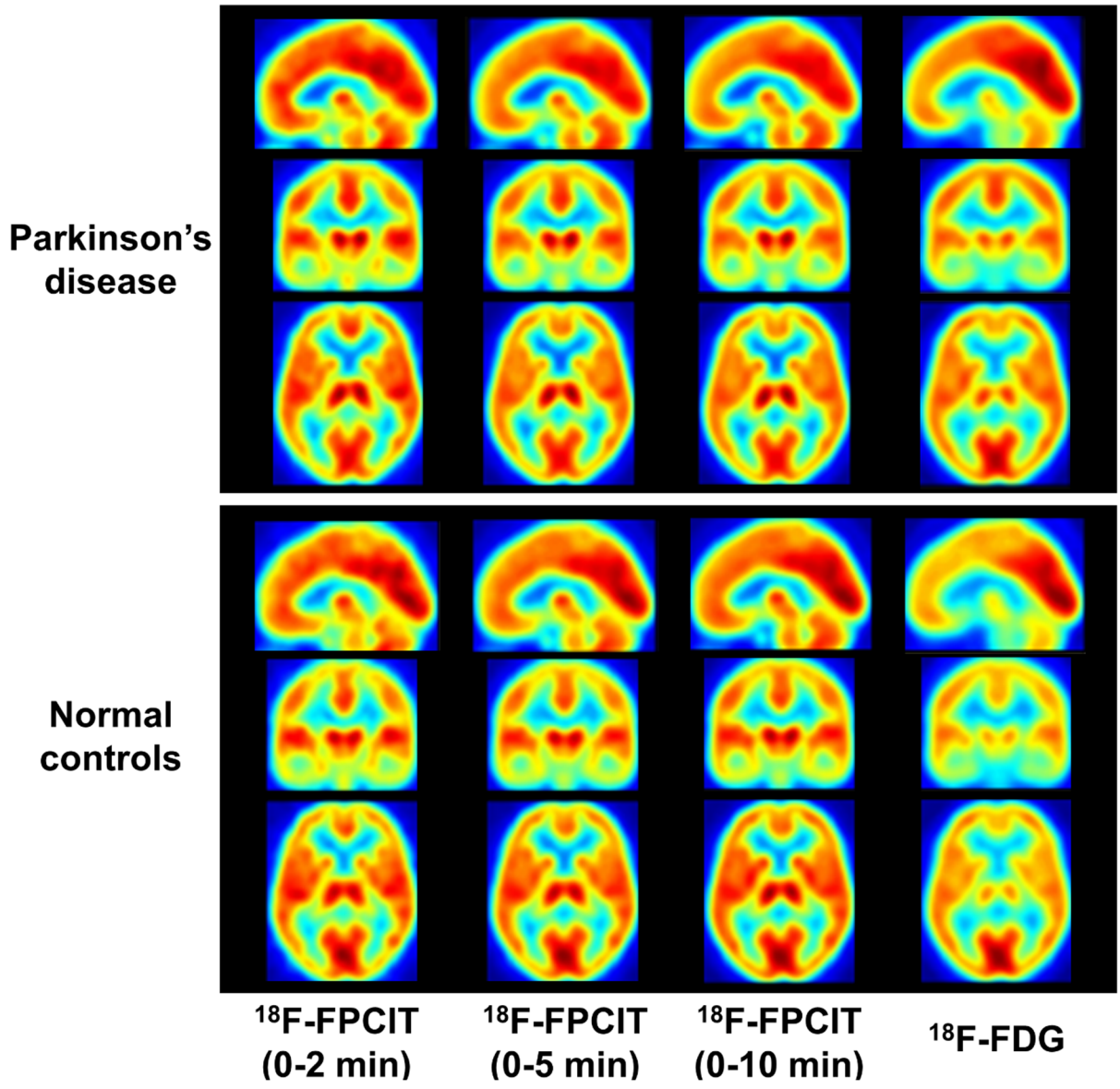

Fig. 1. Mean images in PD patients and normal controls from early-phase ^{18}F-FPCIT and ^{18}F-FDG PET. There was high similarity between the mean images of ^{18}F-FPCIT over the first 2, 5 and 10 min post-injection and the corresponding ^{18}F-FDG images.

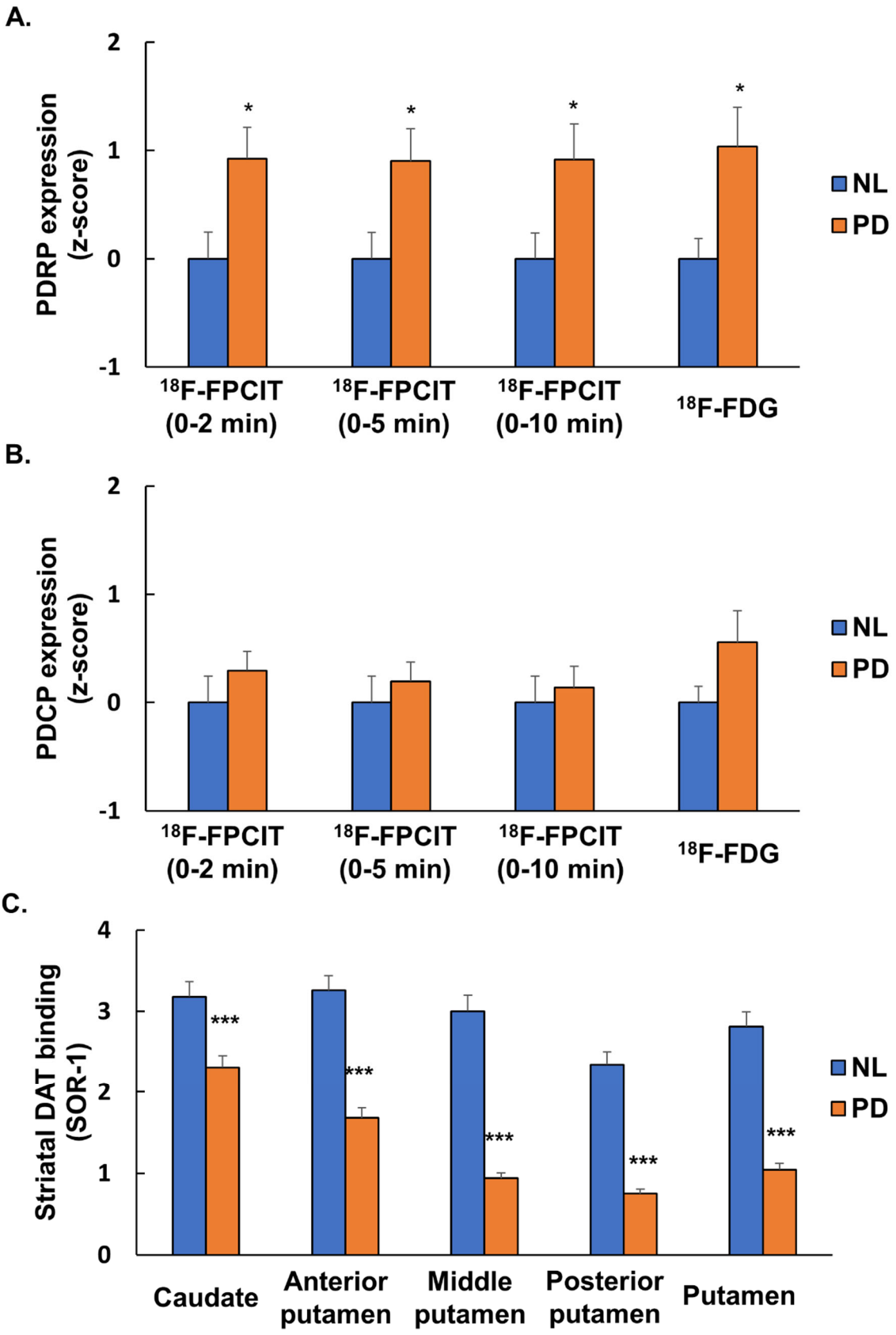
A.
PDRP expression (z-score)
2
1
0
-1
*
*
*
*
NL
PD
18F-FPCIT (0-2 min)
18F-FPCIT (0-5 min)
18F-FPCIT (0-10 min)
18F-FDG
B.
PDCP expression (z-score)
2
1
0
-1
NL
PD
18F-FPCIT (0-2 min)
18F-FPCIT (0-5 min)
18F-FPCIT (0-10 min)
18F-FDG
C.
Striatal DAT binding (SOR-1)
4
3
2
1
0
***
***
***
***
***
NL
PD
Caudate
Anterior putamen
Middle putamen
Posterior putamen
Putamen

Fig.2. Differences in network scores and striatal dopamine transporter (DAT) binding in Parkinson's disease (PD) patients compared to age-matched normal (NL) control subjects. **A/B**. Elevation in PDRP but not PDCP expression values with pseudo CBF images from early-phase ^{18}F-FPCIT PET (0-2 min, 0-5 min and 0-10 min) and metabolic images from ^{18}F-FDG PET respectively. **C**. Reduction in striatal DAT binding in caudate, putamen and its subdivisions from late-phase ^{18}F-FPCIT PET over 90-100 min. PDRP: Parkinson's disease-related pattern; PDCP: Parkinson's disease cognition-related pattern; SOR: striatal-occipital ratio; CBF: cerebral blood flow.

* $P < 0.05$

*** $P < 0.001$ unpaired Student's *t*-tests

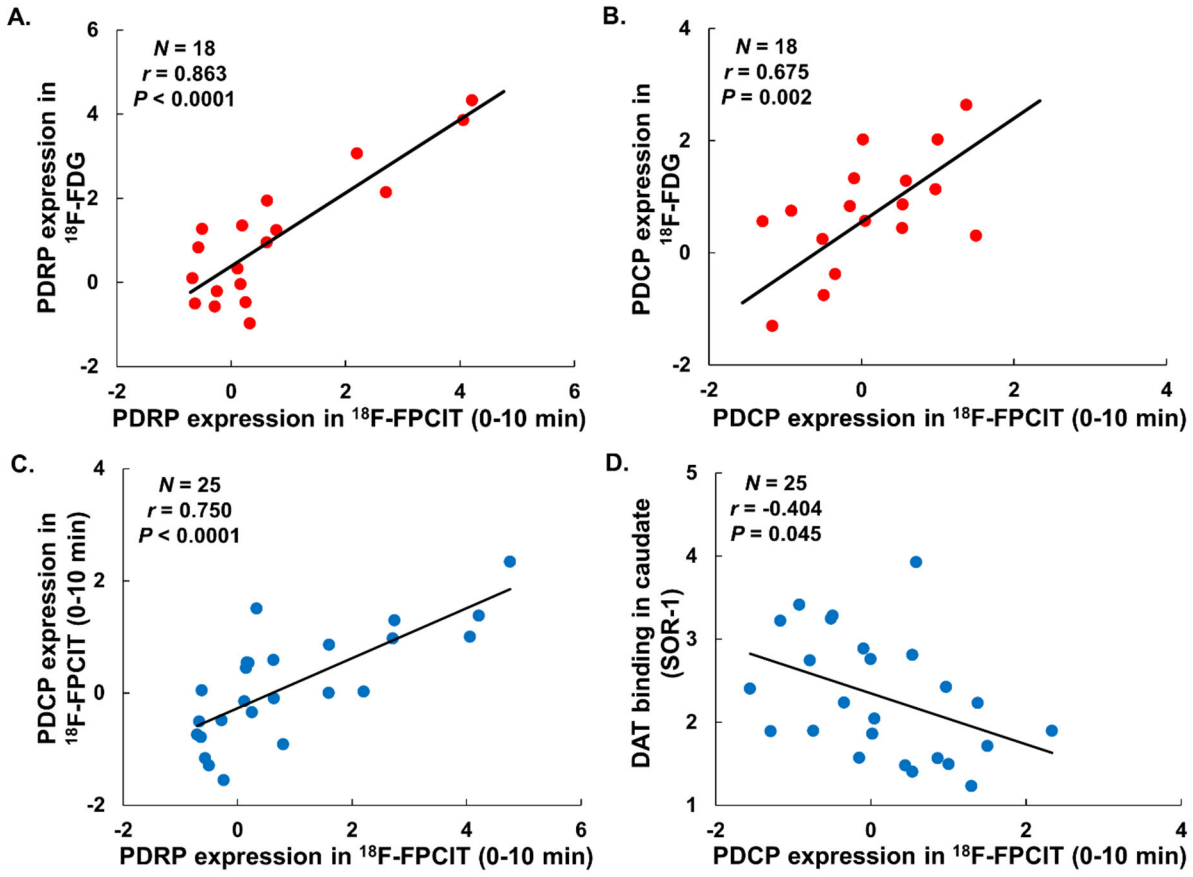

Fig. 3. Correlations in network scores between surrogate CBF images from early-phase ^{18}F-FPCIT and metabolic images in PD patients. **A/B**. PDRP/PDCP expression values computed using ^{18}F-FPCIT PET over 0-10 min correlated closely with those obtained with ^{18}F-FDG PET in the same subjects (PDRP: $r = 0.863$, $P < 0.0001$; PDCP: $r = 0.675$, $P < 0.005$; Pearson correlations). **C/D**. Corresponding PDCP expression values correlated with PDRP expression values ($r = 0.750$, $P < 0.0001$) and DAT binding values in caudate ($r = -0.404$, $P < 0.05$). PDRP: Parkinson's disease-related pattern; PDCP: Parkinson's disease cognition-related pattern; DAT: dopamine transporter; SOR: striatal-occipital ratio; CBF: cerebral blood flow.

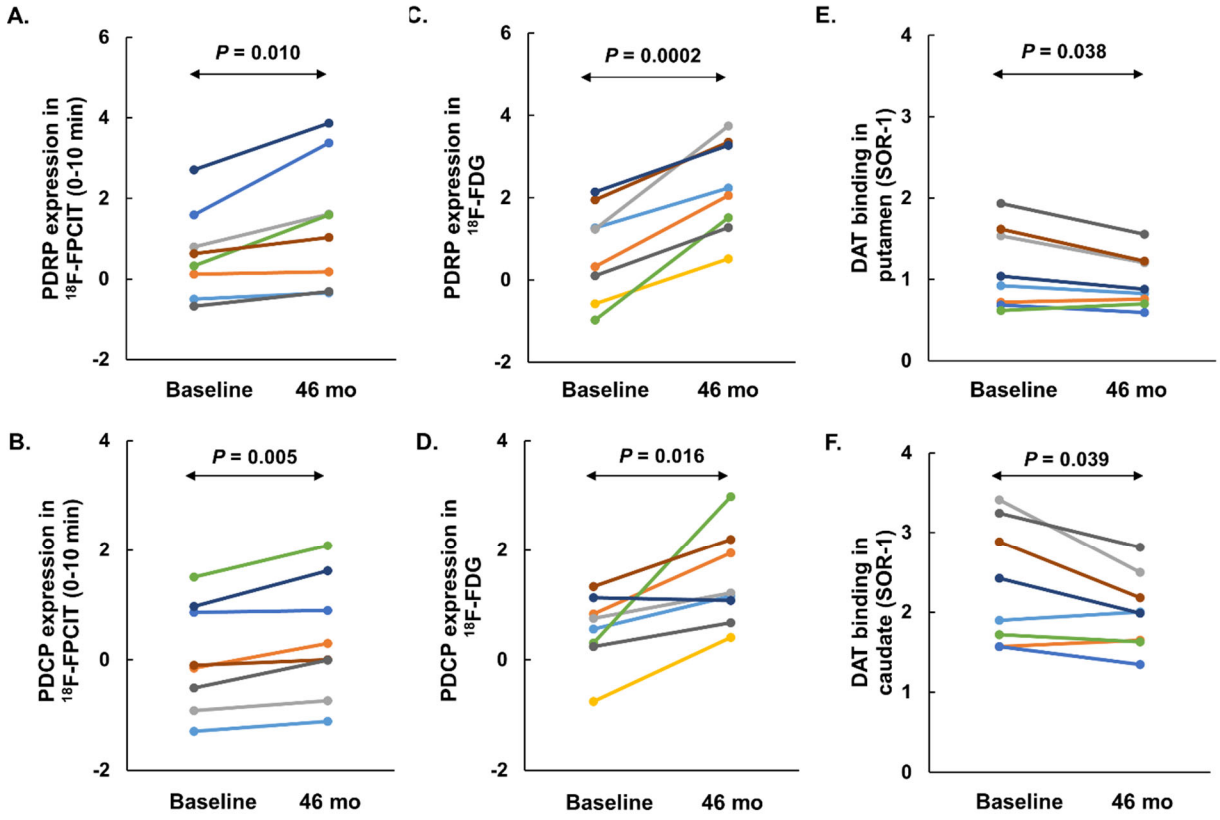

Fig. 4. Longitudinal changes of network scores and striatal DAT binding in PD patients who underwent repeat PET imaging with both ^{18}F-FPCIT and ^{18}F-FDG. **A/B/C/D**. Increases in PDRP/PDCP expression values ($P < 0.02$, paired Student's *t*-tests) with proxy CBF images from early-phase ^{18}F-FPCIT PET over 0-10 min and metabolic images. **E/F**. Reduction in striatal DAT binding ($P < 0.05$) in putamen and caudate from late-phase ^{18}F-FPCIT PET over 90-100 min. [The color codes were the same for 7 PD subjects with dual-tracer data with different colors for two other subjects with either ^{18}F-FPCIT or ^{18}F-FDG PET.] PDRP: Parkinson's disease-related pattern; PDCP: Parkinson's disease cognition-related pattern; DAT: dopamine transporter; SOR: striatal-occipital ratio; CBF: cerebral blood flow.

Graphical Abstract

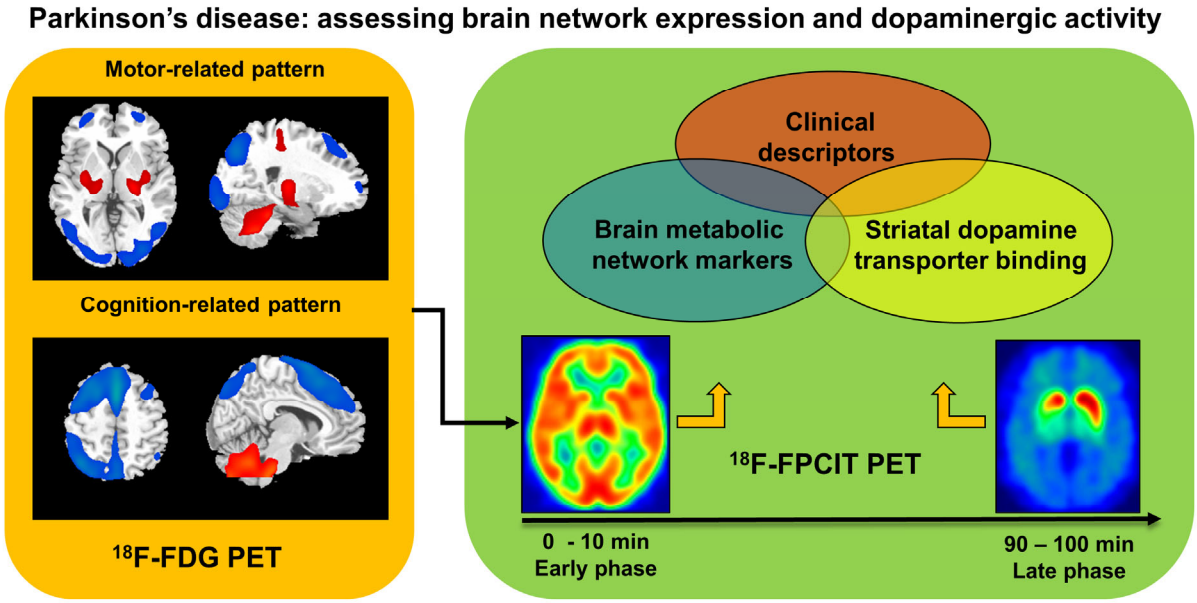

Table 1: Comparisons of PDRP scores at individual frames during early-phase ^{18}F-FPCIT imaging in Parkinson's patients versus normal control subjects and correlations with clinical and ^{18}F-FDG data

PDRP (^{18}F-FPCIT)	1 min	2 min	3 min	4 min	5 min	6 min	7 min	8 min	9 min	10 min
PD vs NL*										
P	0.028	0.034	0.049	0.057	0.034	0.031	0.036	0.046	0.047	0.048
PD2 vs NL*										
P	0.054	0.030	0.023	0.016	0.012	0.010	0.011	0.012	0.013	0.013
PD2 vs PD1#										
P	0.092	0.019	0.011	0.016	0.009	0.005	0.007	0.010	0.009	0.007
Pearson correlation										
UPDRS										
r	0.406	0.435	0.443	0.430	0.446	0.458	0.440	0.420	0.425	0.429
P	0.044	0.030	0.026	0.032	0.026	0.021	0.028	0.037	0.034	0.032
Duration										
r	0.379	0.399	0.411	0.395	0.420	0.440	0.412	0.380	0.391	0.402
P	0.062	0.048	0.041	0.05	0.037	0.028	0.041	0.061	0.053	0.047
PDRP (FDG)										
r	0.702	0.796	0.856	0.872	0.873	0.874	0.873	0.870	0.864	0.857
P	0.001	0.000	0.000	0.000	0.000	0.000	0.000	0.000	0.000	0.000

Data were *P*-values and Pearson correlation coefficients.

PDRP: Parkinson's disease-related pattern; PD: Parkinson's disease; NL: Normal control subjects; UPDRS: the unified Parkinson's disease rating scale. PD1 and PD2 refer to the baseline and 4-year scans of the longitudinal PD group.

* unpaired *t*-tests

paired *t*-tests

Table 2: Comparisons of PDCP scores at individual frames during early-phase ^{18}F-FPCIT imaging in Parkinson's patients versus normal control subjects and correlations with clinical and ^{18}F-FDG data

PDCP (^{18}F-FPCIT)	1 min	2 min	3 min	4 min	5 min	6 min	7 min	8 min	9 min	10 min
PD vs NL*										
P	0.250	0.473	0.637	0.716	0.686	0.654	0.772	0.895	0.874	0.853
PD2 vs NL*										
P	0.906	0.473	0.344	0.344	0.320	0.304	0.324	0.350	0.367	0.386
PD2 vs PD1#										
P	0.334	0.054	0.011	0.007	0.004	0.003	0.001	0.001	0.001	0.002
Pearson correlation										
UPDRS										
r	0.138	0.320	0.343	0.337	0.360	0.378	0.356	0.330	0.334	0.337
P	0.511	0.119	0.093	0.099	0.077	0.063	0.081	0.107	0.102	0.100
Duration										
r	0.467	0.427	0.443	0.451	0.467	0.478	0.436	0.388	0.401	0.412
P	0.019	0.033	0.027	0.024	0.018	0.016	0.029	0.055	0.047	0.041
PDCP (FDG)										
r	0.374	0.611	0.681	0.694	0.684	0.680	0.681	0.675	0.684	0.694
P	0.126	0.007	0.002	0.001	0.002	0.002	0.002	0.002	0.002	0.001

Data were *P*-values and Pearson correlation coefficients.

PDCP: Parkinson's disease cognition-related pattern; PD: Parkinson's disease; NL: Normal control subjects; UPDRS: the unified Parkinson's disease rating scale. PD1 and PD2 refer to the baseline and 4-year scans of the longitudinal PD group.

* unpaired *t*-tests

paired *t*-tests

Table 3: Comparisons of network scores and striatal DAT binding between Parkinson's patients and normal control subjects

PDRP scores	^{18}F-FPCIT (2 min)	^{18}F-FPCIT (5 min)	^{18}F-FPCIT (10 min)	^{18}F-FDG	
PD vs NL*					
P	0.029	0.040	0.030	0.019	
PD2 vs NL*					
P	0.039	0.021	0.014	0.00033	
PD2 vs PD1#					
P	0.043	0.016	0.010	0.00020	
PDCP scores	**^{18}F-FPCIT (2 min)**	**^{18}F-FPCIT (5 min)**	**^{18}F-FPCIT (10 min)**	**^{18}F-FDG**	
PD vs NL*					
P	0.319	0.511	0.658	0.105	
PD2 vs NL*					
P	0.749	0.467	0.396	0.0012	
PD2 vs PD1#					
P	0.792	0.043	0.0051	0.016	
Striatal DAT binding	**Caudate**	**Putamen**	**Anterior putamen**	**Middle putamen**	**Posterior putamen**
PD vs NL*					
P	0.00067	1.4E-08	8.1E-09	6.7E-09	1.2E-08
PD2 vs NL*					
P	0.00056	1.7E-08	1.5E-05	7.4E-09	5.0E-09
PD2 vs PD1#					
P	0.039	0.038	0.063	0.138	0.229

Data were *P*-values.

DAT: dopamine transporter binding; PDRP: Parkinson's disease-related pattern; PDCP: Parkinson's disease cognition-related pattern; PD: Parkinson's disease; NL: Normal control subjects. PD1 and PD2 refer to the baseline and 4-year scans of the longitudinal PD group.

* unpaired *t*-tests

paired *t*-tests

Table 4. Correlations between clinical data and striatal DAT binding values in Parkinson's patients and normal control subjects

		Caudate	Putamen	Ant Putamen	Mid Putamen	Post Putamen
PD (N=25)	UPDRS	-0.156	-0.269	-0.293	-0.311	-0.247
	Duration	-0.361	-0.419 ‡	-0.508 ‡	-0.399 ‡	-0.232
	Caudate		0.798 *	0.877 *	0.721 *	0.594 †
	Putamen			0.929 *	0.968 *	0.849 *
	Ant Putamen				0.881 *	0.657 *
	Mid Putamen					0.871 *
	Post Putamen					
NL (N=16)	Caudate		0.976 *	0.975 *	0.974 *	0.955 *
	Putamen			0.977 *	0.988 *	0.964 *
	Ant Putamen				0.977 *	0.931 *
	Mid Putamen					0.969 *
	Post Putamen					

Data were Pearson correlation coefficients.

DAT: dopamine transporter binding; UPDRS: the unified Parkinson's disease rating scale; PD: Parkinson's disease; NL: Normal control subjects.

* $P < 0.0001$,

† $P < 0.005$,

‡ $P < 0.05$

Table 5. Correlations between PRDP and PDCP scores in Parkinson's patients and normal control subjects

		PDCP			
		^{18}F-FPCIT (2 min)	^{18}F-FPCIT (5 min)	^{18}F-FPCIT (10 min)	^{18}F-FDG
	PDRP				
PD	^{18}F-FPCIT (2 min)	0.664 *	0.715 *	0.692 *	0.586 §
	^{18}F-FPCIT (5 min)	0.621 *	0.724 *	0.727 *	0.663 ‡
	^{18}F-FPCIT (10 min)	0.592 ‡	0.728 *	0.750 *	0.705 †
	^{18}F-FDG	0.217	0.321	0.354	0.713 †
NL	^{18}F-FPCIT (2 min)	0.887 *	0.860 *	0.819 *	
	^{18}F-FPCIT (5 min)	0.879 *	0.899 *	0.885 *	
	^{18}F-FPCIT (10 min)	0.817 *	0.869 *	0.879 *	
	^{18}F FDG				

Data were Pearson correlation coefficients.

PDRP: Parkinson's disease-related pattern; PDCP: Parkinson's disease cognition-related pattern; PD: Parkinson's disease; NL: Normal control subjects.

* $P < 0.0001$,

† $P < 0.001$,

‡ $P < 0.005$,

§ $P < 0.05$

Table 6: Comparisons of network scores between Parkinson' patients and normal control subjects with early-phase ^{18}F-FPCIT PET data

	^{18}F-FPCIT excluding 1st min			^{18}F-FPCIT excluding 1st 2 min		
PDRP scores	**2-2 min**	**2-5 min**	**2-10 min**	**3-5 min**	**3-10 min**	**6-10 min**
PD vs NL*						
P	0.034	0.047	0.034	0.053	0.037	0.040
PD2 vs NL*						
P	0.030	0.018	0.014	0.016	0.013	0.011
PD2 vs PD1#						
P	0.019	0.012	0.009	0.012	0.008	0.007
PDCP scores	**2-2 min**	**2-5 min**	**2-10 min**	**3-5 min**	**3-10 min**	**6-10 min**
PD vs NL*						
P	0.473	0.624	0.728	0.679	0.761	0.809
PD2 vs NL*						
P	0.473	0.365	0.351	0.335	0.340	0.345
PD2 vs PD1#						
P	0.054	0.008	0.002	0.006	0.002	0.001

Data were *P*-values.

PDRP: Parkinson's disease-related pattern; PDCP: Parkinson's disease cognition-related pattern; PD: Parkinson's disease; NL: Normal control subjects. PD1 and PD2 refer to the baseline and 4-year scans of the longitudinal PD group.

* unpaired *t*-tests

paired *t*-tests

Table 7. Correlations between clinical data, PDRP/PDCP scores and striatal DAT binding values in Parkinson's patients

PDRP	UPDRS	Duration	^{18}F-FPCIT (2-2 min)	^{18}F-FPCIT (2-5 min)	^{18}F-FPCIT (2-10 min)
^{18}F-FPCIT (2-2 min)	0.435 §	0.399 §			
^{18}F-FPCIT (2-5 min)	0.441 §	0.409 §	0.987 *		
^{18}F-FPCIT (2-10 min)	0.439 §	0.408 §	0.967 *	0.995 *	
^{18}F-FDG			0.796 *	0.857 *	0.868 *
Striatal DAT binding					
Caudate			-0.268	-0.297	-0.310
Putamen(whole)			-0.300	-0.297	-0.286
Anterior			-0.269	-0.271	-0.264
Middle			-0.353	-0.346	-0.338
Posterior			-0.314	-0.300	-0.293

PDCP	UPDRS	Duration	^{18}F-FPCIT (2-2 min)	^{18}F-FPCIT (2-5 min)	^{18}F-FPCIT (2-10 min)
^{18}F-FPCIT (2-2 min)	0.320	0.427 §			
^{18}F-FPCIT (2-5 min)	0.343	0.451 §	0.983 *		
^{18}F-FPCIT (2-10 min)	0.347	0.437 §	0.959 *	0.993 *	
^{18}F-FDG			0.611 ‡	0.675 †	0.685 †
Striatal DAT binding					
Caudate			-0.347	-0.385	-0.379
Putamen(whole)			-0.296	-0.302	-0.275
Anterior			-0.338	-0.353	-0.331
Middle			-0.337	-0.338	-0.315
Posterior			-0.251	-0.244	-0.227

Data were Pearson correlation coefficients.

PDRP: Parkinson's disease-related pattern; PDCP: Parkinson's disease cognition-related pattern; DAT: dopamine transporter binding; UPDRS: the unified Parkinson's disease rating scale. The shaded areas indicate the correlations that were no longer significant after removing the first 1-min frame.

* $P < 0.0001$,

† $P < 0.005$,

‡ $P < 0.01$,

§ $P < 0.05$

Table 8. Correlations between clinical data, PDRP/PDCP scores and striatal DAT binding values in Parkinson's patients

PDRP	UPDRS	Duration	^{18}F-FPCIT (3-5 min)	^{18}F-FPCIT (3-10 min)	^{18}F-FPCIT (6-10 min)
^{18}F-FPCIT (3-5 min)	0.441 §	0.410 §			
^{18}F-FPCIT (3-10 min)	0.438 §	0.408 §	0.996 *		
^{18}F-FPCIT (6-10 min)	0.435 §	0.405 §	0.991 *	0.999 *	
^{18}F-FDG			0.869 *	0.871 *	0.869 *
Striatal DAT binding					
Caudate			-0.305	-0.313	-0.317
Putamen(whole)			-0.295	-0.283	-0.276
Anterior			-0.271	-0.263	-0.257
Middle			-0.342	-0.335	-0.331
Posterior			-0.294	-0.289	-0.286

PDCP	UPDRS	Duration	^{18}F-FPCIT (3-5 min)	^{18}F-FPCIT (3-10 min)	^{18}F-FPCIT (6-10 min)
^{18}F-FPCIT (3-5 min)	0.348	0.455 §			
^{18}F-FPCIT (3-10 min)	0.349	0.436 §	0.994 *		
^{18}F-FPCIT (6-10 min)	0.348	0.424 §	0.986 *	0.998 *	
^{18}F-FDG			0.688 †	0.688 †	0.684 †
Striatal DAT binding					
Caudate			-0.395	-0.381	-0.372
Putamen(whole)			-0.302	-0.272	-0.254
Anterior			-0.355	-0.328	-0.313
Middle			-0.335	-0.311	-0.297
Posterior			-0.240	-0.223	-0.213

Data were Pearson correlation coefficients.

PDRP: Parkinson's disease-related pattern; PDCP: Parkinson's disease cognition-related pattern; DAT: dopamine transporter binding; UPDRS: the unified Parkinson's disease rating scale. The shaded areas indicate the correlations that were no longer significant after removing the first 2-min or 5-min frames.

* $P < 0.0001$,

† $P < 0.005$,

§ $P < 0.05$

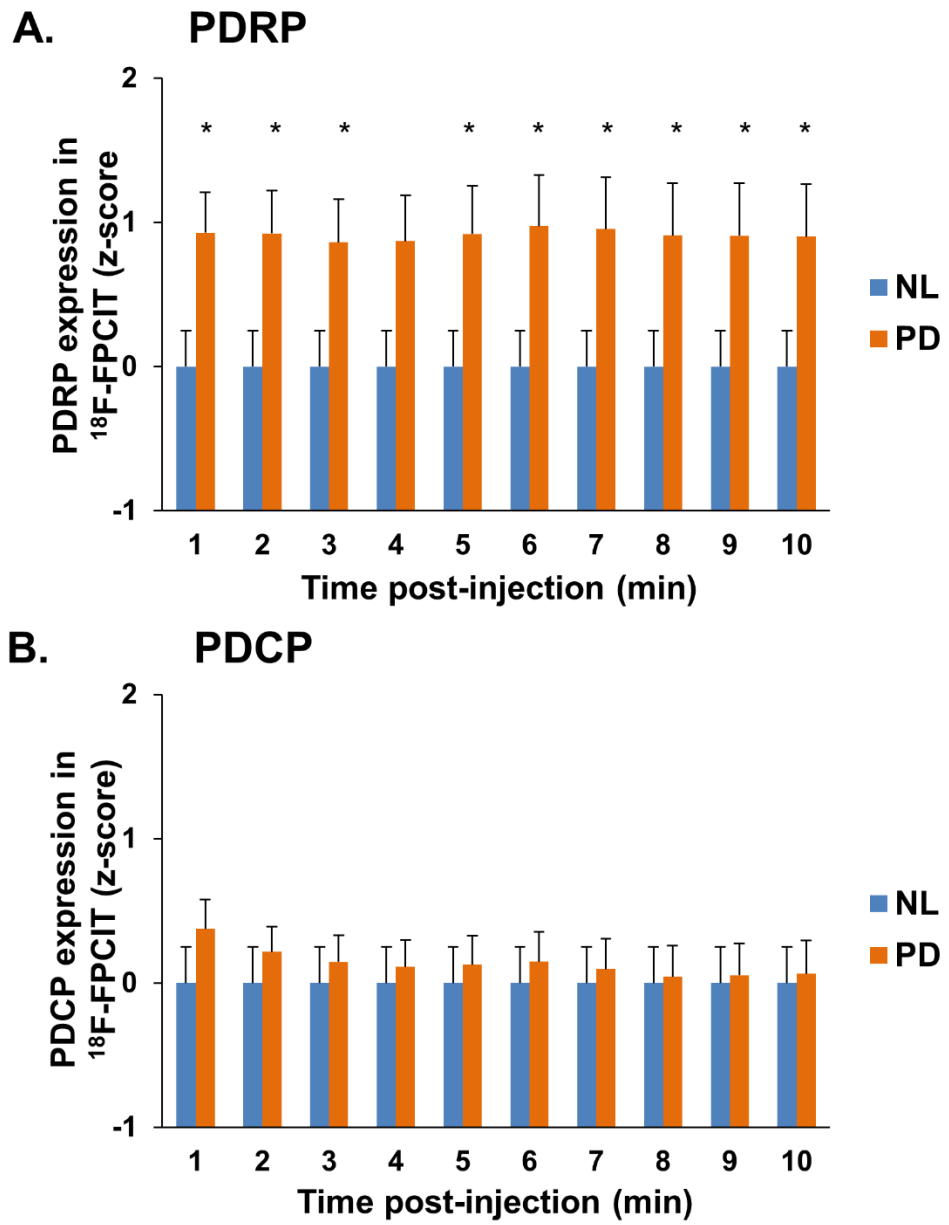

Fig. 1. Differences in network scores in Parkinson's disease (PD) patients compared to age-matched normal (NL) control subjects. PDRP (**A**) but not PDCP (**B**) expression values were elevated with pseudo blood flow images from early-phase ^{18}F-FPCIT PET at individual 1-min frames over 0-10 min post-injection. PDRP: Parkinson's disease-related pattern; PDCP: Parkinson's disease cognition-related pattern.

* $P < 0.05$ unpaired Student's *t*-tests

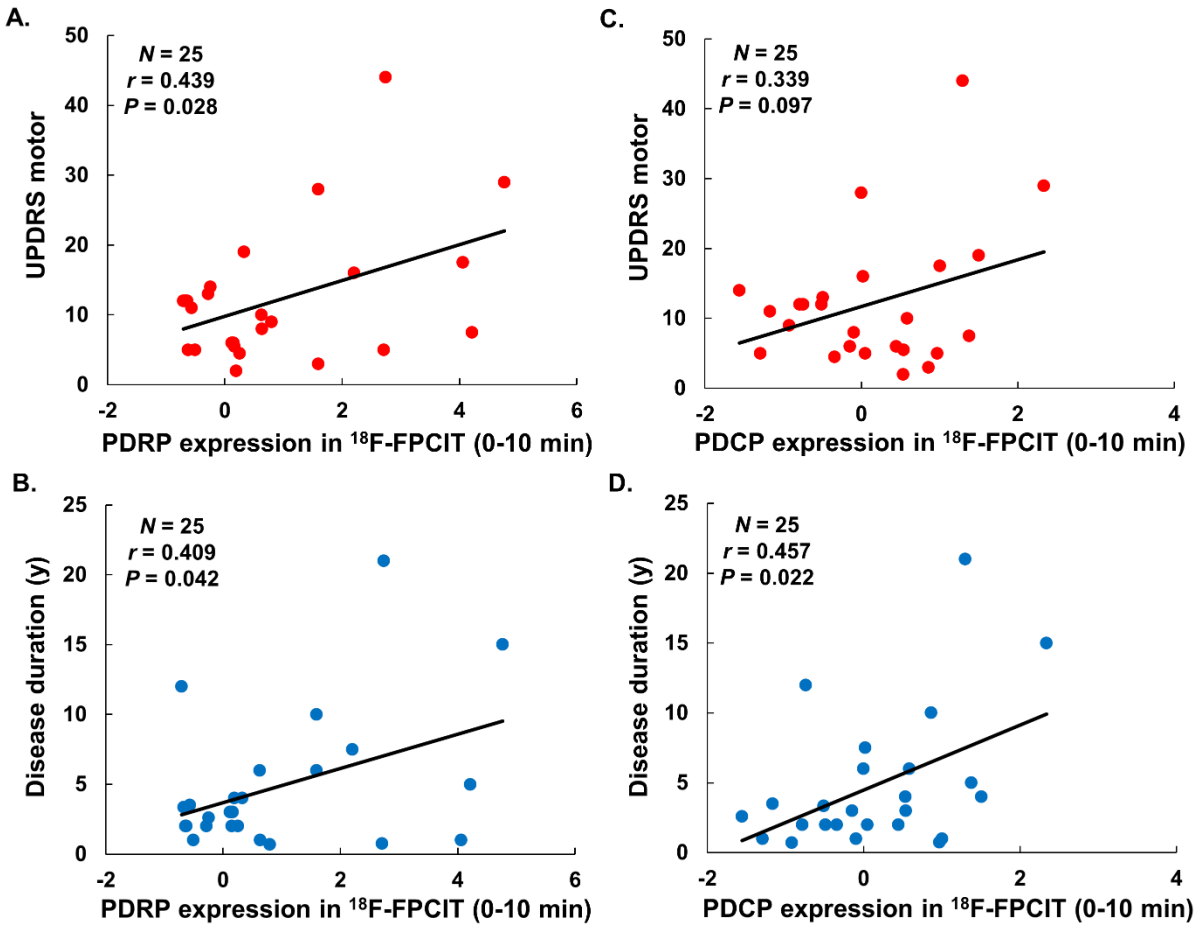

Fig. 2. Correlations between clinical measures and network scores using proxy CBF images from early-phase ^{18}F-FPCIT PET in PD patients. **A/B**. PDRP expression values computed in ^{18}F-FPCIT scans over 0-10 min correlated with UPDRS motor ratings (r = 0.439, P < 0.05; Pearson correlation) and disease duration (r = 0.409, P < 0.05). **C/D.** Corresponding PDCP expression values correlated not with UPDRS motor ratings (r = 0.339, P = 0.10) but with disease duration (r = 0.457, P < 0.05). PDRP: Parkinson's disease-related pattern; PDCP: Parkinson's disease cognition-related pattern; UPDRS: the unified Parkinson's disease rating scale; CBF: cerebral blood flow.

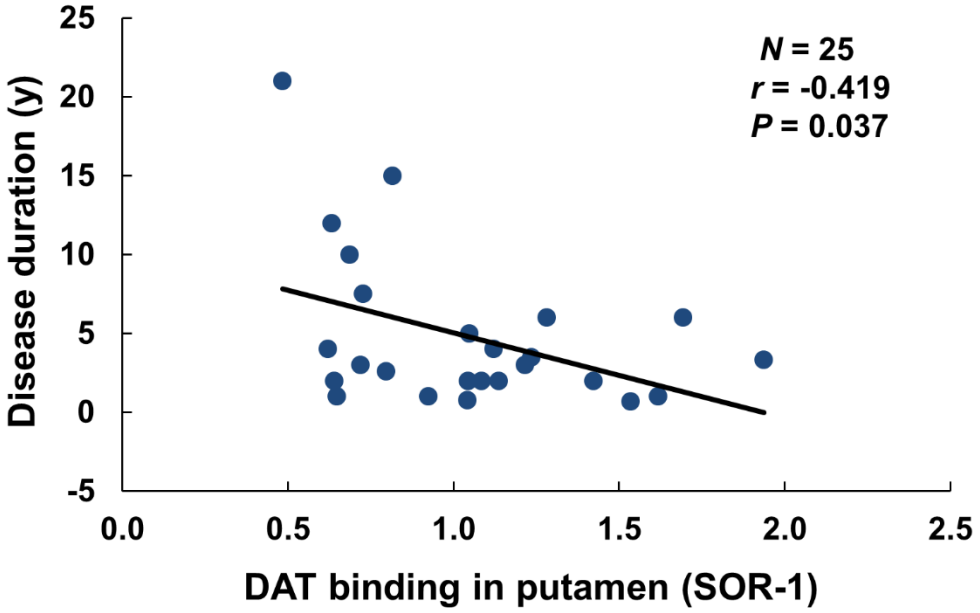

Fig. 3. Correlations between dopaminergic marker and clinical measure in 18F-FPCIT PET images. Disease duration in PD patients correlated negatively with DAT binding values in putamen obtained in late-phase 18F-FPCIT scans (r = -0.419, P = 0.037). PD: Parkinson's disease; DAT: dopamine transporter binding; SOR: striatal-to-occipital ratio.

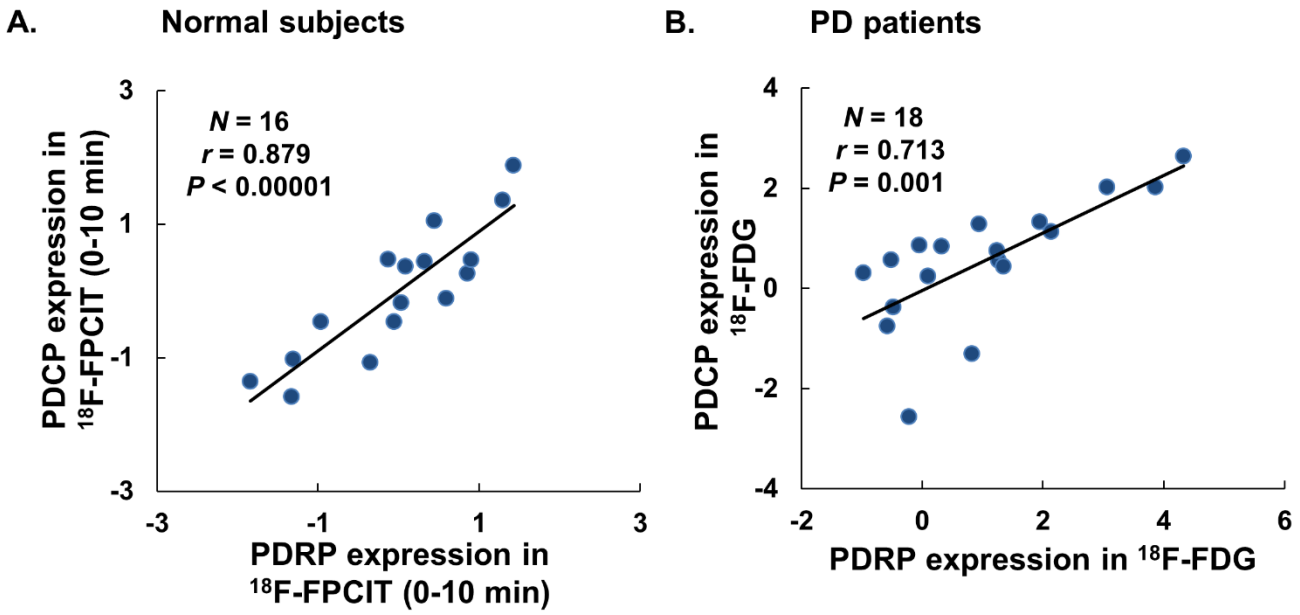

Fig. 4. Correlations between network markers in ^{18}F-FPCIT and ^{18}F-FDG PET images. **A.** PDCP scores measured in surrogate CBF images from early-phase ^{18}F-FPCIT PET correlated closely with analogous PDRP scores in normal control subjects (r = 0.879, P < 0.0001). **B.** Corresponding PDCP and PDRP scores computed in ^{18}F-FDG scans correlated in PD patients (r = 0.713, P = 0.001). PDRP: Parkinson's disease-related pattern; PDCP: Parkinson's disease cognition-related pattern; CBF: cerebral blood flow; PD: Parkinson's disease.

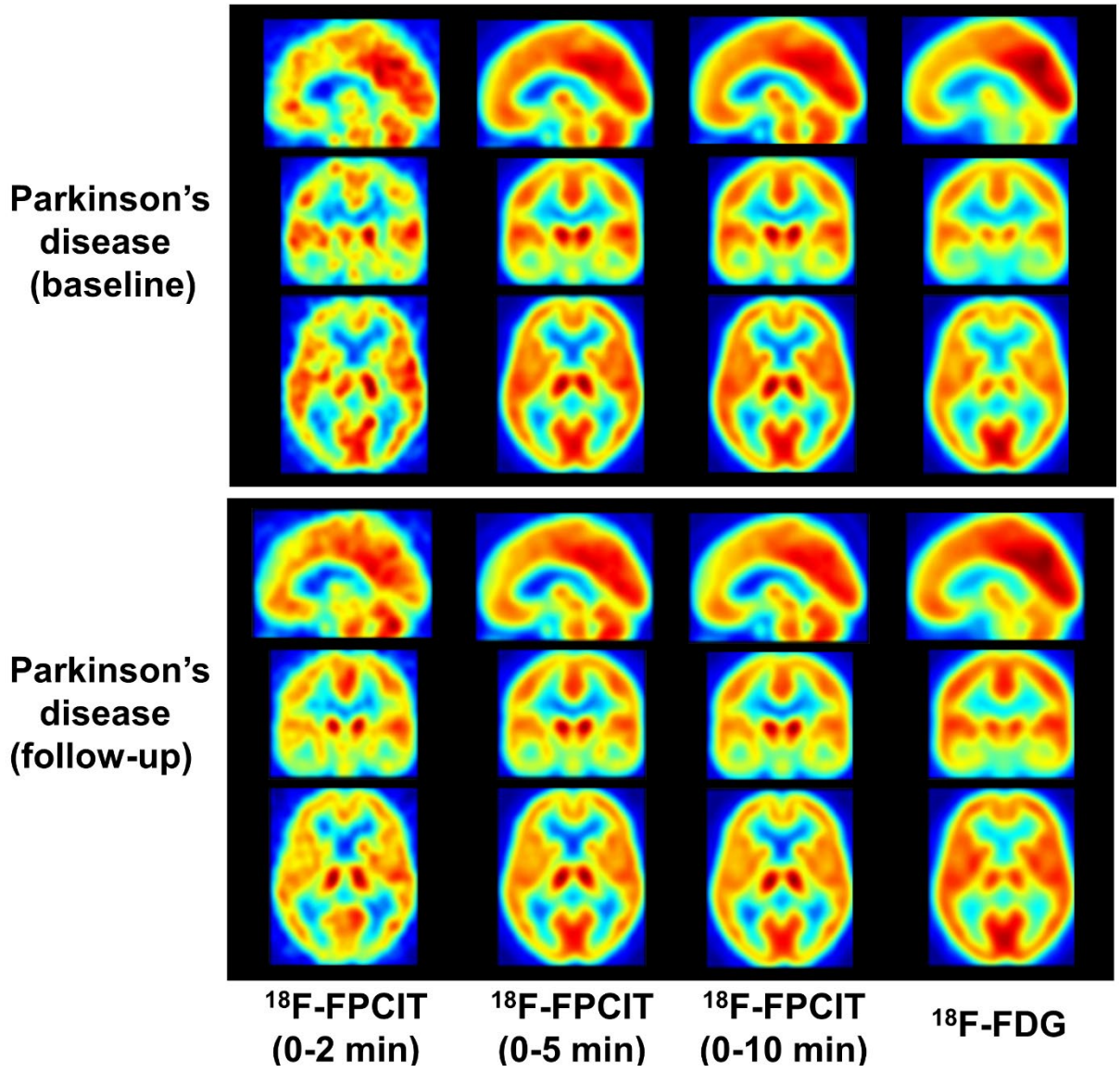

Fig. 5. Mean images in PD patients at baseline and follow-up from early-phase ^{18}F-FPCIT and ^{18}F-FDG PET scans. There was high similarity between the mean images of ^{18}F-FPCIT over the first 2, 5 and 10 min post-injection and the corresponding ^{18}F-FDG images.